NEUROSCIENCE
RESEARCH ARTICLE

Shirin Vafaei Shooshtari et al. / Neuroscience 406 (2019) 510–527

Confidence Representation of Perceptual Decision by EEG and Eye Data in a Random Dot Motion Task

Shirin Vafaei Shooshtari,[a] Jamal Esmaily Sadrabadi,[a] Zahra Azizi[b] and Reza Ebrahimpour[a,c,*]

[a]*Department of Computer engineering, Shahid Rajaee Teacher Training University, Tehran, Iran*

[b]*Institute for Cognitive Science Studies, Tehran, Iran*

[c]*School of Cognitive Sciences, Institute for Research in Fundamental Sciences (IPM), Tehran, Iran*

Abstract—The Confidence of a decision could be considered as the internal estimate of decision accuracy. This variable has been studied extensively by different types of recording data such as behavioral, electroencephalography (EEG), eye and electrophysiology data. Although the value of the reported confidence is considered as one of the most important parameters in decision making, the confidence reporting phase might be considered as a restrictive element in investigating the decision process. Thus, decision confidence should be extracted by means of other provided types of information. Here, we proposed eight confidence related properties in EEG and eye data which are significantly descriptive of the defined confidence levels in a random dot motion (RDM) task. As a matter of fact, our proposed EEG and eye data properties are capable of recognizing more than nine distinct levels of confidence. Among our proposed features, the latency of the pupil maximum diameter through the stimulus presentation was established to be the most associated one to the confidence levels. Through the time-dependent analysis of these features, we recognized the time interval of 500–600 ms after the stimulus onset as an important time in correlating features to the confidence levels.

Key words: decision making, confidence, EEG, eye data, time-dependent analysis.

INTRODUCTION

Decision making is one of the most important aspects of human life. Environmental evidence could be gathered by the neural population of the brain's perceptual system (Kim and Shadlen, 1999; Shadlen and Newsome, 2001; Gold and Shadlen, 2007; Shadlen and Kiani, 2013). When the neural activities of this population reach a certain value, decisions will be made (Gold and Shadlen, 2002; Roitman and Shadlen, 2002; Kiani et al., 2008). The mentioned evidence's affection in cognitive processing could be monitored by means of different modularity. Neurophysiology investigations have confirmed that the firing rates of selective neurons have a direct relationship with the evidence strength (Mazurek et al., 2003; Huk and Shadlen, 2005; de Lafuente et al., 2015). EEG signals have also demonstrated a similar direct relationship to the evidence strength. Accordingly, the buildup rate of EEG signals in the centro-parietal area of the brain has a correlation with the motion strength in an RDM task (O'Connell et al., 2012; Kelly and O'Connell, 2013, 2015). Moreover, eye movement parameters, specifically saccade, show a significant inverse correlation with the stimulus strength (Shadlen and Newsome, 2001).

Real-life decision making frequently is followed with no obvious feedback about the quality of a taken decision (Van den Berg et al., 2016b). In this manner, decision confidence is a valuable and vital source of decision outcome which could be considered as an estimated feedback for decisions (Bahrami et al., 2012; Purcell and Kiani, 2016; Van den Berg et al., 2016b). This decision attribute has been subjected to many decision making discussions (Kepecs et al., 2008; Kiani and Shadlen, 2009; Fetsch et al., 2014; Navajas et al., 2014; Kubanek et al., 2015; Folke et al., 2016; Hebart et al., 2016; Samaha et al., 2017) which attempts to explain confidence behavior by different types of data.

Behavioral, computational and neurophysiological data have demonstrated that choice certainty has a strong correlation with both accuracy and reaction time (RT) of a decision (Balakrishnan and Ratcliff, 1996; Kiani and Shadlen, 2009; Fetsch et al., 2014; Van den Berg et al., 2016a). While the relationship between accuracy and confidence has been broadly accepted by researchers (Yeung and Summerfield,

*Corresponding author. Tel.: +982122970060x2501.
E-mail address: rebrahimpour@srttu.edu (Reza Ebrahimpour).

Abbreviations: EEG, electroencephalography; RDM, random dot motion; DDM, drift diffusion model; ERP, event related potential ERP; Pe, error positivity; RT, reaction time; ICA, independent component analysis; LIP, lateral intraparietal cortex; FEF, frontal eye field; CSD, current source density; SEM, standard error of the mean; SVM, support vector machine.

https://doi.org/10.1016/j.neuroscience.2019.03.031
0306-4522/

2012; de Gardelle and Mamassian, 2014; Drugowitsch et al., 2014; Hebart et al., 2016), there is also evidence for the causal role of the RT in the confidence formation (Kiani et al., 2014). Furthermore, the drift diffusion model (DDM) has been widely and successfully applied to the performance and statistics of the RT in human decision making (Ratcliff and Smith, 2004; Bogacz et al., 2006; Van den Berg et al., 2016b). Accordingly, although some studies discussed the complexity of confidence and furthermore introduced innovative solutions to fit confidence data to the DDM (Moreno-Bote, 2010; Drugowitsch and Pouget, 2012; Yeung and Summerfield, 2012), however, there are also studies endeavored to find and demonstrate the classic DDM parameters in correlation with certainty level (Ratcliff and Starns, 2009, 2013; Philiastides et al., 2014).

EEG data which record the electrical activity of the brain has also contributed to the study of decision confidence. EEG studies have confirmed that choice certainty emerges as early as the onset of the stimulus in the event-related potential (ERP) of signals so that amplitude of the signals varies across confidence levels (Zizlsperger et al., 2014). In addition, the single trial analysis indicated the discrimination between certain and uncertain signals, which gradually increases until the report of the decision. This observation could suggest that confidence forms during the decision process (Gherman and Philiastides, 2015). Moreover, a relationship between error judgment and confidence has been observed in EEG signals after reporting the decision. Post-decisional confidence ratings and error detection share the same mechanism; thus, the amplitude of the signals pertinent to positive error (pe) varies based on the level of confidence (Boldt and Yeung, 2015).

The certainty of a decision as one of the considerable cognitive attributes of the decision making could be directly analyzed via the eye data. Studies have revealed that saccade latency and saccade trajectory deviation respectively decreases and increases while evidence strength in RDM task increases (McSorley et al., 2014). Moreover, it has been recently shown that microsaccade can impact decision formation in EEG signals (Loughnane et al., 2018). Lempert et al. carried out a study on the eye data and confidence value in an auditory task and observed that the pupil diameter had a straight correlation with the levels of confidence (Lempert et al., 2015). Gaze fixation, as an important event in the analysis of the eye data, has been shown to have a direct correlation with choice certainty. Confidence has been reported to vary according to the time of target presentation in a detection letter task when the subject has to fixate his/her gaze (Navajas et al., 2014). Generally, although, the EEG and eye data have been employed in decision making studies extensively, there are fewer investigations about the confidence interaction with extracted data from these two aspects.

Often, in perceptual decision making experiments, decision confidence is obtained by the report of a subject admitted about how much a decision is correct (Kiani et al., 2014; Zizlsperger et al., 2014; Heereman et al., 2015). Meanwhile, in some other experiments, it is recommended not to interfere with the decision making process by requesting subjects to report their confidence (Van den Berg et al., 2016b). Consequently, when a subject performs a sequential, multi-stage or discrete decision making task, it is suggested to skip the confidence report between stages of the decision. In this way, it is interesting to estimate confidence in these situations by means of some modularity.

Here, we exploited eight confidence features from the combination of the EEG and eye data, comparing and ranking them based on their convoyed information related to the confidence levels which were confirmed to have different associations to the classic RDM parameters. The best two of our proposed properties were the maximum peak latency of EEG signals and the pupil diameter's positive peak latency which had the highest correlation with the confidence. our EEG time dependent analysis have shown the time interval of 500–600 ms after the stimulus onset as an important time period, which might be arguably pertinent to the confidence formation.

METHODS

Participants

Fourteen participants (four females; all right-handed; aged between 21 and 37 years) performed our RDM task. Data from four of the participants excluded because of either excessive noise in EEG electrodes crucial to analysis or repetitive difficulty in eye monitoring phase which consequently affected the behavioral data as well. The experiment was approved by the ethics committee of the Iran University of Medical Sciences. All the participants had a normal or corrected-to-normal vision, and none of them had any history of psychiatric and neurological diagnosis. They engaged in several training sessions in which they became familiar with the task.

Design and procedures

In our experiment, the participants had to indicate the predominant motion direction in a cloud of moving dots (up or down). The participants were seated in an adjustable chair in a semi-dark room with chin and forehead supported in front of a CRT display monitor (17 inches; PF790; refresh rate, 75 Hz; screen resolution, 800 × 600; viewing distance, 57 cm).

In our RDM task, each trial began with the appearance of a red fixation point (diameter 0.3°) at the center of the display. After 300 ms of the participant's fixation, two choice-targets appeared on the top and downside of the screen with 8° eccentricity corresponding to the two possible motion directions (up and down) (Fig. 1A). Each target was shaped as a gradient rectangle (9° length and 0.5° width), letting the participants specify their certainty on a scale of uncertain to certain (left to right; red to green). The stimulus was presented within a 5° circular aperture at the center of the screen after a short random delay (200–500 ms, truncated exponential distribution). The participants indicated their responses by saccadic eye movement to the chosen target as soon as possible while the degree of certainty was determined by the horizontal endpoint of the subject's saccade (Fig. 1A). Accordingly, they were also required to maintain their gaze

on the bar for 500 ms to determine their decision and confidence value. After the gaze moved away 2.8° from the center, the stimulus was extinguished and the RT of the trial recorded. The paradigm of the experiment was similar to previous work (Kiani et al., 2014).

The motion stimulus was what utilized and has been described in detail in the previous study (Shadlen and Newsome, 2001). Both direction and strength of the motion changed randomly trial by trial. Motion coherence was chosen from the following six values: 0%, 3.2%, 6.4%, 12.8%, 25.6%, and 51.2%. The subjects completed a session involving four blocks. There were 200 trials in every block; the coherence levels were randomly selected from the six coherence levels, equally resulting in at least 33 trials of each coherence level in every block. The experiment presentation code was written in PsychToolbox (Brainard and Vision, 1997).

Responses had to be completed within five seconds; distinctive auditory feedback (Beep Tones) was provided for correct and incorrect responses. The type of feedback of 0% coherence trials was selected accidentally by a uniform distribution. The RT was calculated from the motion stimulus onset until the main saccade initiation. The EEG and eye data were recorded continuously as the experiment proceeded.

In addition to the main experiment, we established two post-experiment versions of the task, in each of which, two of the subjects participated. The first post-experiment was the same version of RDM, with the only difference that at the beginning of each trial, a set of completely random motion dots for 500 ms was presented (Zizlsperger et al., 2014) and then it shifted to the coherent motion. Therefore, sensory-evoked EEG potentials at early stimulus onset were eliminated.

In the second post-experiment, red circles (0.5° diameter) were substituted for gradient target bars and the participant indicated their two levels of certainty by the means of different keys. In this task design, by eliminating the saccadic report, we evaluated the amplitude of the EEG signals that reached a certain value in response time.

Behavioral data analysis

Altogether, 8000 trials were collected from 40 experimental blocks in the main experiment. Confidence was calculated by dividing the horizontal endpoint of saccade into three equal portions (Kiani et al., 2014; Van den Berg et al., 2016a,b). The left portion was taken as low confidence level while the right and middle portion were considered as high and mid confidence levels, respectively. The probability of correct response, the RT and confidence against motion strength was calculated and plotted (Fig. 1B-D).

Additionally, in order to verify our behavioral data, RT and accuracy data were fitted to a drift diffusion model (Ratcliff and Rouder, 2000; Ratcliff and McKoon, 2008). The fitting procedure which we used was the fast-dm toolbox with Kolmogorov-Smirnov (KS) and maximum likelihood criteria for the optimization method (Voss and Voss, 2007; Voss et al., 2013). Moreover, in order to study the parameters of the fitted model in three conditions of high, mid and low confidence, we fitted the data of each level to the model in various conditions; we evaluated the variation of drift rate, boundary separation, starting point and none decisional time to the confidence levels across the subjects. In every evaluation, we considered the remaining parameters as constant. Absolute values of all the parameters were reported while none decisional time was represented in seconds.

Recording, pre-processing and analyzing EEG data

We used a 32-channel amplifier for the EEG signal recording (eWave, produced by ScienceBeam, http://www.sciencebeam.com/) which provided 1K sample/s of time resolution (Karimi-Rouzbahani et al., 2017a, 2017b). EEG was recorded at 31 scalp sites (Fp1, Fp2, AF3, AF4, C3, C4, P3, P4, O1, O2, F7, F8, T7, T8, P7, P8, FPz, Fz, Cz, Pz, Oz, POz, FC1, FC2, CP1, CP2, FC5, FC6, CP5, CP6). The EEG signals were referenced to the right mastoid and the earth electrode to the left mastoid.

The recorded data were taken to Matlab (http://mathworks.com) and pre-processed as follows. The signals were first digitally notch-filtered in the range of 45–55 Hz for AC power frequency noise removal. In addition, they were filtered using a band-pass filter from 0.1 Hz to 35 Hz (Zizlsperger et al., 2014) for removing high frequency and cognitive independent noises. Muscle and eye-blink artifacts were removed from the signals using the independent component analysis (ICA) as implemented in EEGLAB (Delorme and Makeig, 2004). To select the removable ICA component, ADJUST plugin (Mognon et al., 2011) was used.

In order to explore EEG data, single trials and ERPs data were analyzed. ERPs were measured by averaging single trials of all the subjects. We employed the signal of CP1, CP2, Cz and Pz channels for our analysis. We epoched the EEG data, i.e. stimulus-aligned channel activities from 100 ms pre-stimulus to 800 ms post-stimulus. Then, these epochs were baselined to a window -100 ms to stimulus-locked to prevent differences in the visual response to the stimulus affecting the baseline. In addition, response-aligned analyses were epoched from 600 ms pre-response to 100 ms post-response. Here, the epochs were baselined to a window between -600 ms to -500 ms related to the response-locked.

The ERP signals were examined for each level of confidence and by means of them and single trial analysis; a number of features were extracted. Here, features with a stronger correlation with confidence were reported.

As a mean to find the best time when the EEG signal showed the most significant relationship to confidence, the decoding method was utilized (Cichy et al., 2014; Karimi-Rouzbahani et al., 2017a, 2017b). This analysis performed a classification task (in this case, the support vector machine (SVM)) on three levels of confidence based on the specific part of every single trial (in this case, 100 ms window). Step size was set to 5 ms, meaning that in every 5 ms through the latency of the signals, decoding analysis was performed. In this way, in every 5 ms, we had 100 samples of the EEG data for every single trial which was labeled by the reported confidence level. The SVM performed on this temporal dataset. For classification evaluation, we used the leave one out cross validation method. This method considered all expect one of the

observation records (N-1 (N as the number of the records)) as the training set. The remaining one considered as the test set. This treatment was repeated for the total number of the observations which consequently all of the records considered as the test set exactly once. Putting together all of the test results, we could reach the accuracy of EEG signals in the recognition of three confidence levels in this specific time period. Clearly, accuracy more than chance level corresponded to the valuable information about the confidence. 95% confidence interval of 200 runs was shown in decoding figures (Fig. 5) for better assessment.

Eye data recordings

The Eye data were collected using an EyeLink 1000 (SR-Research). This device allowed a 1000-Hz sampling rate. A chin and forehead rest was used to stabilize the participants' heads. The system was controlled by a dedicated host PC, and then was calibrated and validated by presenting nine targets at the center, edges, and corners of the display monitor before data collection. Data of the left eye was recorded and passed to the host PC via an Ethernet link during data collection. The average accuracy of the system was 0.25–0.5° and operated in a pupil-corneal reflection mode.

An eye tracker recorded the position of the eyes on the x- and y-axis and pupil diameter. In addition, this system can detect eye movement events such as fixation, saccade, blink and so on. Characteristics of the eye data were studied, and a number of features were extracted. Here, features with stronger correlation with confidence were reported.

Analyzing eye and EEG Features

Our observations on EEG signals motivated us to extract related features to the confidence levels form signals (Fig. 4). First EEG feature is the slope of the EEG signals from 300 ms after the onset of the stimulus until the signals reach to its peak (Maximum value). The second feature is the maximum amplitude of the signals in the same time period. In the other word, this feature represented the value of the signal's amplitude in the time of signal peak. Third one is the Alpha band of the signal in the same mentioned time period. We transferred the signal amplitude into the frequency domain by Fourier Transformation. Then we summed the returned signals' power in the frequency period of 8 Hz to13 Hz. Fourth feature is the latency of the EEG signal positive peak. Time of the positive peak after 300 ms after the onset of the stimulus had been considered as the 4th EEG feature.

We also extract four features (Fig. 7) from eye data. First eye feature is the slope of the pupil diameter signal from the onset of the stimulus until the saccade initiation toward one of the targets. Second one is the latency of the pupil diameter signal positive peak. In fact, the time of the maximum value of the pupil diameter's signals had been considered as one of the Eye features. Third eye feature is the normalized number of the fixations while the stimulus is presented. Fourth feature is pupil diameter at the time of response.

For better evaluation of our extracted features, we also isolated the effect of coherence and RT altogether. In this analysis – due to low number of trials- we used the trials with coherence of 12.8% and 6.4% (Zizlsperger et al., 2014) which have same RT distribution – 600–750 ms. As the matter of fact, RTs of three confidence levels in the mentioned subset of data did not show any statistic difference ($H(2) = 1.74$, $P = .41$). Confidence is expected to vary less in this situation. Note we refer to this dataset as Same RT subset. Moreover, we used a single trial analysis for better assessment of our prospered features (Fig. 8A).

Statistical analysis

Statistical comparisons were performed in Matlab, using Kruskal–Wallis test. Note features' data did not significantly follow a normal distribution (Anderson-Darling test), hence, we used the non-parametric tests. In behavioral data, we used this test to determine the significant differences between psychometric function thresholds (α parameter) and chronometric function for each level of confidence (n = number of samples was 10, df = degree of freedom was 2). For this purpose, we included all subject data in three confidence levels (for both RT and probability Correct analysis). For DDM fitted parameters, the data from nine participants compared in three groups corresponding to each level of confidence (n = 9 df = 2). 95% confidence interval for each parameter of three levels of confidence was measured using 10,000 bootstrap replications (Fig. 2). Kruskal–Wallis test was also used in the analysis of the proposed features (Figs. 4 and 7; for all the analysis n = 10, df = 2). Additionally, we evaluated the features' representative capability in the one level coherence and SameRT subset with the same statistical test (Kruskal–Wallis n = 10, df = 2); We also conducted Kruskal-Wallis test on single trial data which their results summed up in Fig. 8A. Note in Fig. 8A in AllCoh n = 7645 and df = 2, in 12.8 n = 1263 and df = 2 and finally for SameRT n = 497 and df = 2. Since our Statistical comparisons were done in three groups, we also applied the Dunn test as a post hoc procedure in all above analyses to evaluate the significant difference of each level to others. The results of these pairwise comparisons were presented in the Appendix A section.

RESULTS

Behavioral results

Fourteen subjects performed an RDM task in which they simultaneously reported the perceived direction of dots and their confidence by saccadic eye movement to the target. Since the evidence strength has been reported to be correlated to the accuracy and decision time (Palmer et al., 2005; Hanks et al., 2006; Churchland et al., 2008; Zylberberg et al., 2016), we expected to observe higher accuracy and faster RT while increasing motion strength. The psychometric functions were plotted by applying a cumulative Weibull function on the subject's behavioral data (Quick, 1974). There are two parameters in this function. The discrimination

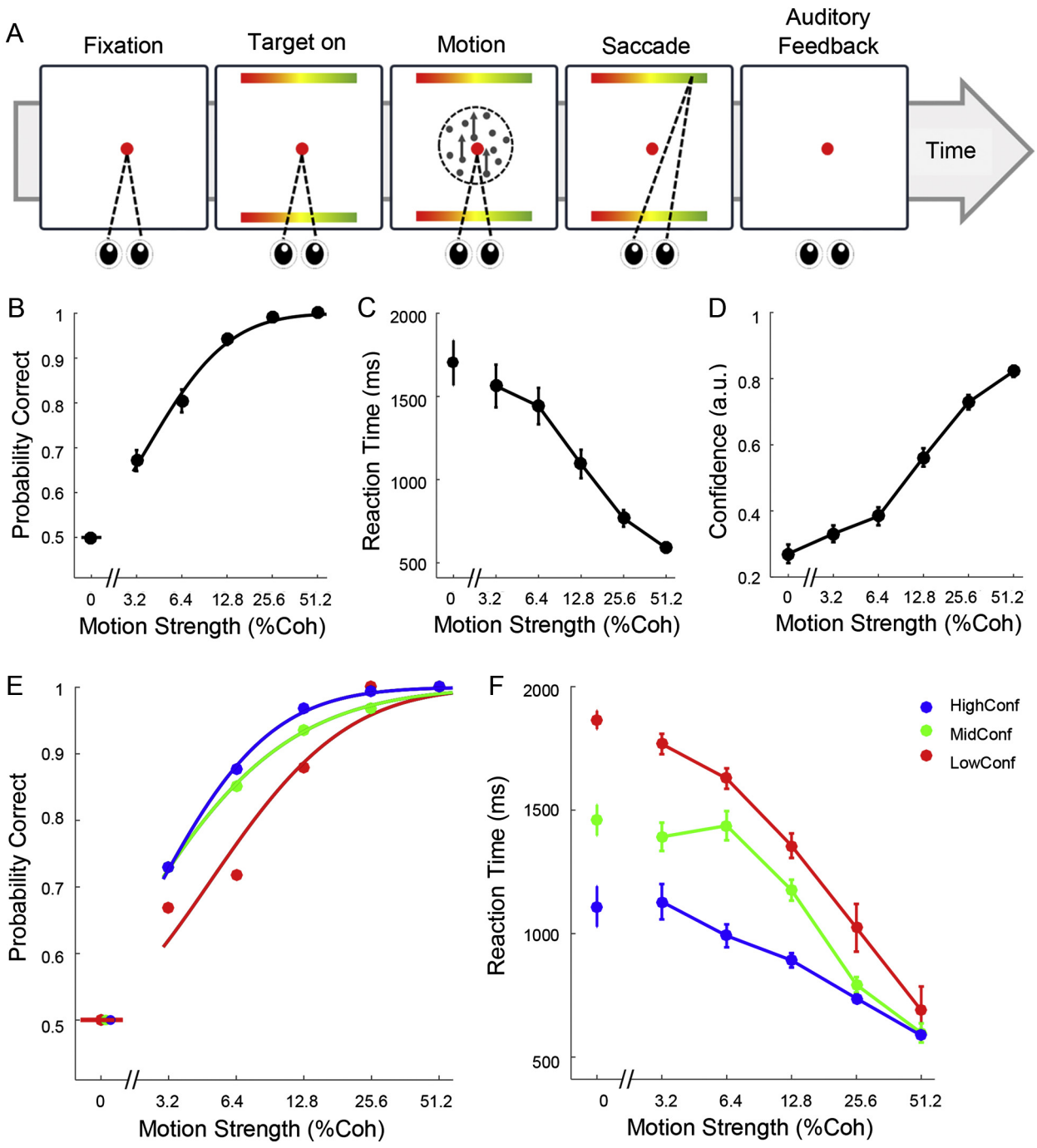

Fig. 1. Behavioral analysis: (A) The main experiment in which the subjects had to indicate their decision and confidence at the same time by saccadic eye movement. **(B)** The psychometric function where dots represent the mean of the subject accuracy in different coherence (α = 6.72, β = 1.17), higher coherence is followed by higher accuracy, error bars show a reverse correlation with motion strength. The fitted line is the fitted cumulative Weibull function. **(C)** The chronometric function where dotes are the average reaction time of all data in a specific coherence, higher coherence is led by the faster response and vice versa. The error bar decreases with an increase of motion coherence. **(D)** The reported confidence where dots show the average of the reported confidence value scaled from 0 to 1 in every coherence. **(E)** The psychometric function for the three levels of confidence where higher confidence is followed by higher accuracy and the trends are maintained properly according to the confidence levels. **(F)** The chronometric function for each level of confidence where higher confidence is followed by a faster reaction time. The error bars are SEM in all the plots.

threshold (α) is the coherence level at which the subject would make 82% correct choices. The second parameter, β, describes the slope of the psychometric function at the point of α (Roitman and Shadlen, 2002). Based on the performance results, the subjects shared more correct trials in higher motion strengths (Fig. 1B).

Our data verified a reverse relationship between the RT and motion strength (Reinagel, 2013), as shown in Fig. 1C. In

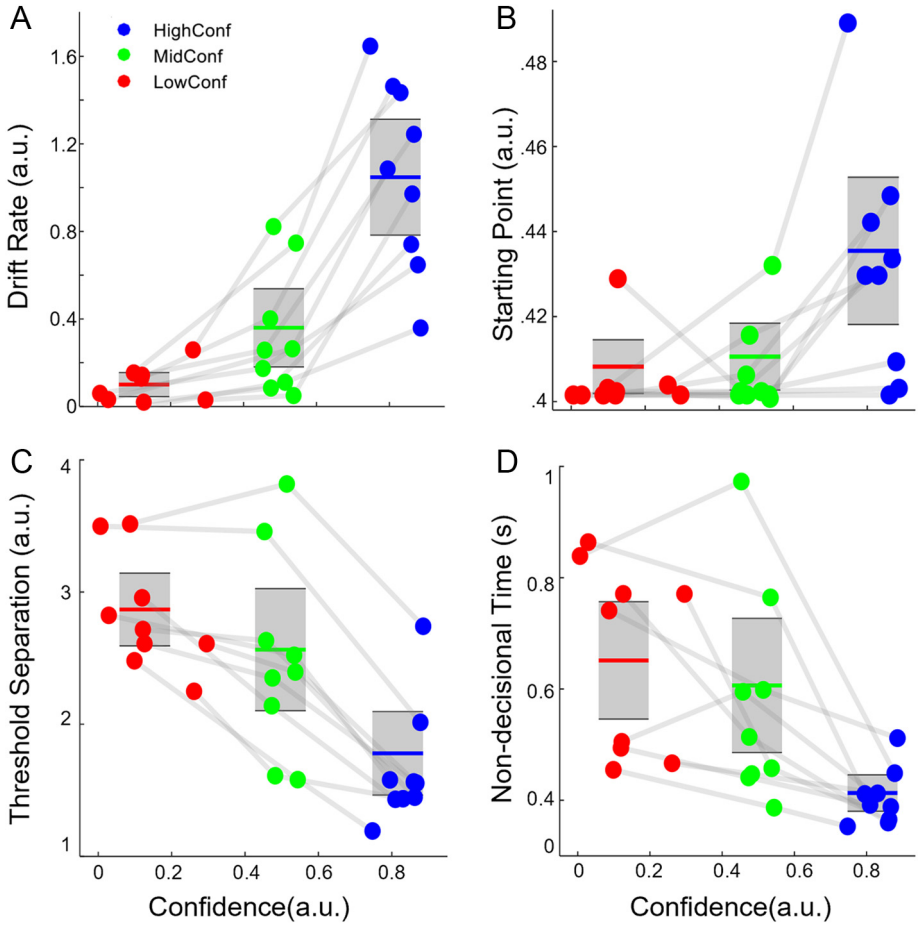

Fig. 2. DDM fitted parameters. (A) The drift rate of the DDM was significantly different in the three levels of confidence. **(B)** The starting point of the DDM, similar to the drift rate, significantly differed in the confidence levels. **(C)** The difference in the threshold separation of the DDM was significant in the levels of confidence. **(D)** Finally, the none decisional constant of the DDM expressed significant difference among the levels of confidence too. Each data point represented a participant in one of the three possible levels of confidence. The grey box was the confidence interval of 10,000 bootstrap replications of each parameter. The horizontal lines were the mean of each parameter.

another representation, we exposed the reported confidence versus motion coherence. Similar to the effect of coherence on accuracy, confidence had a strong correlation with motion strength (Baranski and Petrusic, 1998; Kiani and Shadlen, 2009; Fetsch et al., 2014) (Fig. 1D). However, the slight difference between probability correct and reported confidence as a function of motion strength (Fig. 1B and D) reveals the destructive effect of the RT on confidence. In other words, in high levels of coherence (25.6% and 51.2%), the performance was highly identical whereas the confidence values were more diverse. Based on these observations, it could be inferred that the reason was the diversity of response time (Petrusic and Baranski, 2003; Kiani et al., 2014).

It was highly vital for our study to ensure that the subjects had perceived the concept of confidence so that they could declare their confidence levels accurately. So we additionally analyzed the trials belonging to each of the three confidence levels. As is illustrated in Fig. 1E,F, the performance and RT was highly diverse in these levels. The Kruskal–Wallis test (see method) showed a significant reverse relationship between the value of α and level of the confidence (α = 9.17, 5.45, 4.89 for low, mid and high confidence level, respectively, $H(2) = 9.86$, $P = .007$). To examine the variation of RT with confidence, we plotted RT in six levels of coherence within three levels of confidence. As the result demonstrated in Fig. 1F, each level of confidence differed in RT distinctively ($H(2) = 19.74$, $P < .001$; Fig. 1F). (See Table A.1 in Appendix A section for post hoc tests).

To verify the data, we fitted the accuracy and RT data to a DDM model. The model well fitted the participants' psychometric and chronometric functions (Kolmogorov-Smirnov P-value = .52) (Voss et al., 2013). However, the interpretation of this P-value might be challenging and statistically significant misfits could be expected (Ratcliff et al., 2004; White et al., 2009). Therefore, Monte-Carlo simulations were applied to overcome the biases of P-values from statistical model tests (Clauset et al., 2009; Voss et al., 2013). This validation showed that synthetic datasets and our original model were not significantly different in the goodness of fit (ΔBIC < 6). According to these two assessments, it was likely that our data could be sufficiently fitted to the DDM model.

To assess the relation of behavioral data and levels of confidence, we fitted all behavioral data of nine out of the ten subjects (due to the high RT of one of the participants) to a drift-diffusion model across three levels of confidence. By repeating data fitting several times, each time letting only one parameter to vary, the DDM model parameters (a, v, z, t0) for three confidence levels were calculated. Fig. 2 shows 95% of the confidence interval of 10,000 bootstrap replications for each level of confidence.

The Kruskal–Wallis test showed significant differences between the drift rates of the three levels of confidence across the subjects ($H(2) = 17.45$, $P < .001$; Fig. 2A). The Kruskal–Wallis test of the threshold separation ($H(2) = 13.08$, $P = .001$; Fig. 2B) and the non-decisional constant time ($H(2) = 12.54$, $P < .001$; Fig. 2C) demonstrated a significant difference. Moreover, the starting point ($H(2) = 9.17$, $P = .01$; Fig. 2D) showed a less significant difference between the three levels of confidence.

To outcast the role of coherence on the observed effects (Fig. 2), the declared procedures were further applied to data of one level coherence (12.8%). Although the statistical results were weakened for all the four

parameters, we could still see a significance difference in drift rate ($H(2) = 8.27$, $P = .01$), non-decisional constant time ($H(2) = 7.17$, $P = .03$), starting point ($H(2) = 6.96$, $P = .03$) and the threshold separation ($H(2) = 7.98$, $P = .02$) from DDM fitted to one level of coherence and confidence (see Table B.1 in Appendix A section for post hoc tests).

EEG features

As the first step, we analyzed the EEG data to identify the confidence formation and then by evaluating the signals, we extracted a number of features correlated to confidence. Here, we derived the ERP of averaged signals for three levels of confidence to verify whether there was a significant difference in the centro-parietal area across levels of confidence similar to the observed behavior in coherence levels (Kelly and O'Connell, 2013).

Fig. 3A,C-E exhibits all the subjects' ERPs for confidence levels time-locked to the stimulus onset in different conditions. The first negative peak, N1 (about 100 ms post-stimulus onset), was similar to what was reported in cell recording data from primates where the activity of neurons (firing rate) decreased only after the onset of stimulus (Roitman and Shadlen, 2002). The second peak which was about 200 ms post-stimulus in ERP signals was due to the sudden representation of the stimulus (Kelly and O'Connell, 2013). In the post-experiment results section, a brief argument was mounted related to this peak. The most important peak in our results was P300 that increased in 300–600 ms after the onset of the stimulus. Some of the previous studies found P300 at the heart of the framework of decision-making in the human brain (Rohrbaugh et al., 1974; Twomey et al., 2015). Indeed, immediately after its discovery in 1965, the centro-parietal "P300" or "P3b" component was connected to decision making and degree of uncertainty (Sutton et al., 1965). In addition, findings reflected the P300 role in the encoding of confidence which is caused by accumulated evidence (Urai and Pfeffer, 2014). Hence, we suspected that this period might be highly informative to the confidence levels whose information lies in some features of the signals which need to be extracted.

Analyzing ERP signals, we observed three factors expressively related to the level of confidence. The first one was the slope of a fitted line to the ERP signal in a window from 300 ms post-stimulus to the positive peak of the signal. Based on the brought ERP in Fig. 3A, the slope of ERP signals differed in each level so that higher confidence signal resulted in steeper slope; here the slope of the ERPs related to the mid and low confidence levels respectively decreased rather than high confidence signal.

The second factor was the signal amplitude at the time of the main positive peak. The amplitude of the signals in all the three confidence levels increased over time but the highest peak latency was observed around 500 to 600 ms after the stimulus onset. A previous neurophysiology study established (Kiani and Shadlen, 2009) that firing rates of lateral intraparietal cortex (LIP) neurons were higher in the certain situation comparing to uncertain conditions. We also observed a significant relationship between the signal amplitude and levels of confidence in our result; high confidence had the largest amplitude as compared to the other levels of confidence. This result was also supported with topography analysis. The brain topography was obtained based on the amplitude of the signals with respect to the reference (right mastoid) where high to low amplitudes were represented with the red to blue color range. In Fig. 3F-H, scalp maps are shown in each level of confidence in the centro-parietal area so that the high confidence signals had the highest activity (more red color) whereas the low confidence signals had the lowest activity (less red color), which is resulted by more amplitude for high confidence levels compared to the other levels.

As the third factor, we can mention the main positive peak latency in the ERP signals. In ERP of high confidence signals, the amplitude reached its maximum value earlier that two other confidence levels. Low confidence signals tended to reach their maximum value later than higher confidence ones. Consequently, mid confidence positive peak latency would be set between the latency of high and low confidence signals. This treatment is detectable in Fig. 3A.

Previous study distinguished the correlation between buildup rate of signals and coherence in centro-parietal area (Kelly and O'Connell, 2013), Their main effect was evident in our work as well so that high coherence resulted in the steeper slope (Fig. 3B). Since coherence is the strong characteristic of confidence (Baranski and Petrusic, 1998; Van den Berg et al., 2016b), it seems essential to inspect whether the discrimination between the confidence levels was due to the existence of different coherences. To evaluate this possibility, we accomplished the same analysis in one constant coherence level. We chose the coherence rate of 12.8% because we expected enough trials for each level of confidence in this coherence level (Zizlsperger et al., 2014).

Fig. 3. ERP analysis. (A) ERPs in the three levels of confidence where the ramping activities after 300 ms of the stimulus onset, dependent slope and the peak latency were correlated to the confidence levels. **(B)** ERPs for coherence levels where the signals were quite similar to the confidence levels. Coherence levels were able to successfully separate from each other in the centro-parietal area of the brain. **(C)** ERPs of the confidence levels in one coherence level where the signal related to the confidence levels was separated in this situation. This observation outcast the dependency of the confidence to the coherence. The observed factors in the previous ERP were recognizable in this analysis as well. **(D)** ERPs of the confidence levels in the correct trials where the confidence level signals were separated in this condition which eliminated the influence of accuracy on these signals. The mentioned features were also apparent in this analysis. **(E)** ERPs of the confidence levels in the Same RT subset of 12.8% and 6.4% coherencies where the discrimination and treatment of the signals did not change in this analysis. **(F-H)** The scalp topography in EEG recording relevant to low, mid and high confidence from left to right, respectively, in the time interval of 300–600 ms. High confidence had more activity compared to the other two confidence levels. The color bar shows the amplitude of the activity. The shaded areas are the SEM.

Analyzing one level of coherence, we can still observe a distinction in the signals of the three confidence levels and also all the factors listed above (Fig. 3C).

To support the fact that our findings are not relevant to subject performance, we analyzed the ERP signals in the three levels of confidence only for correct

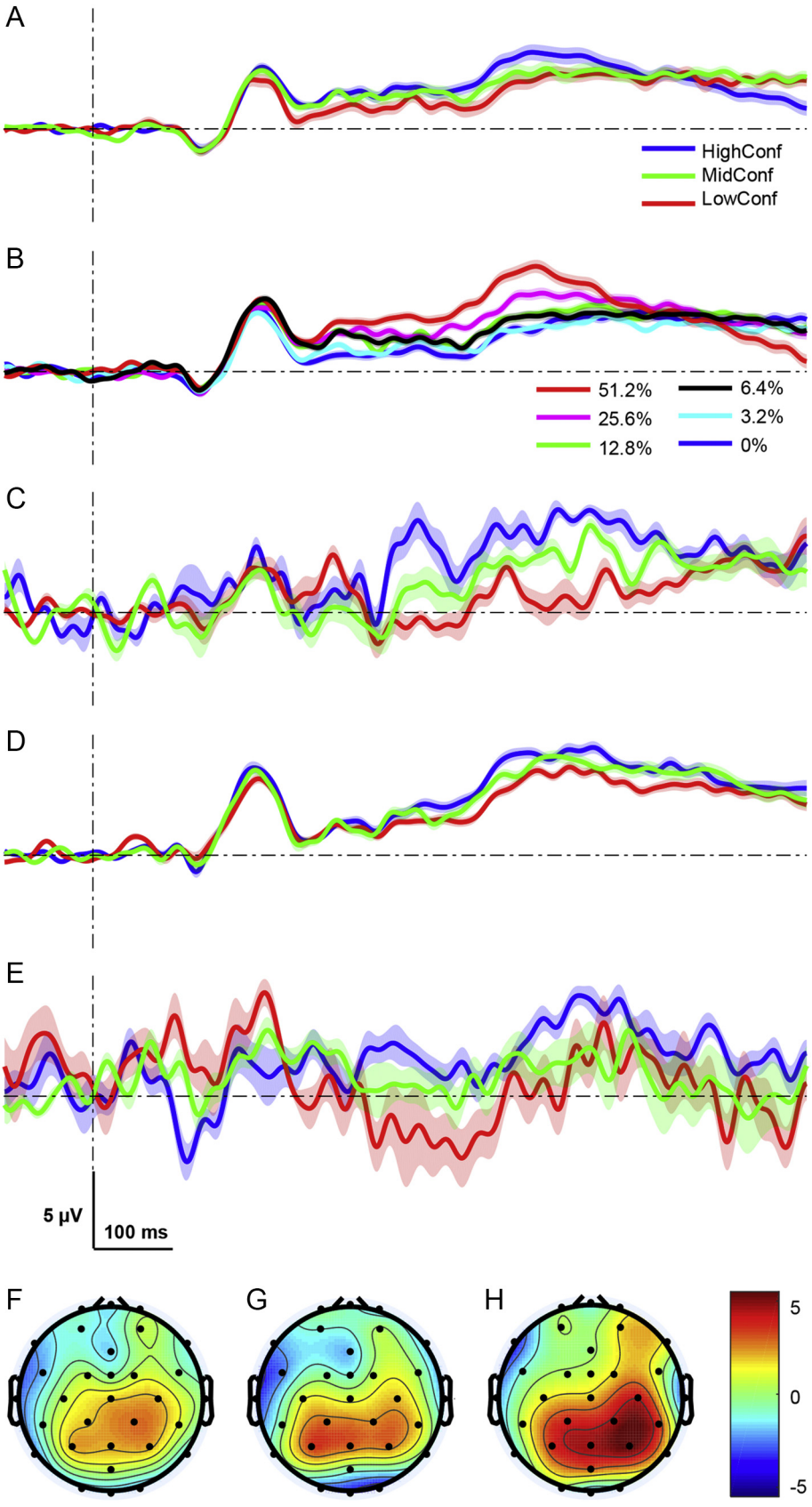

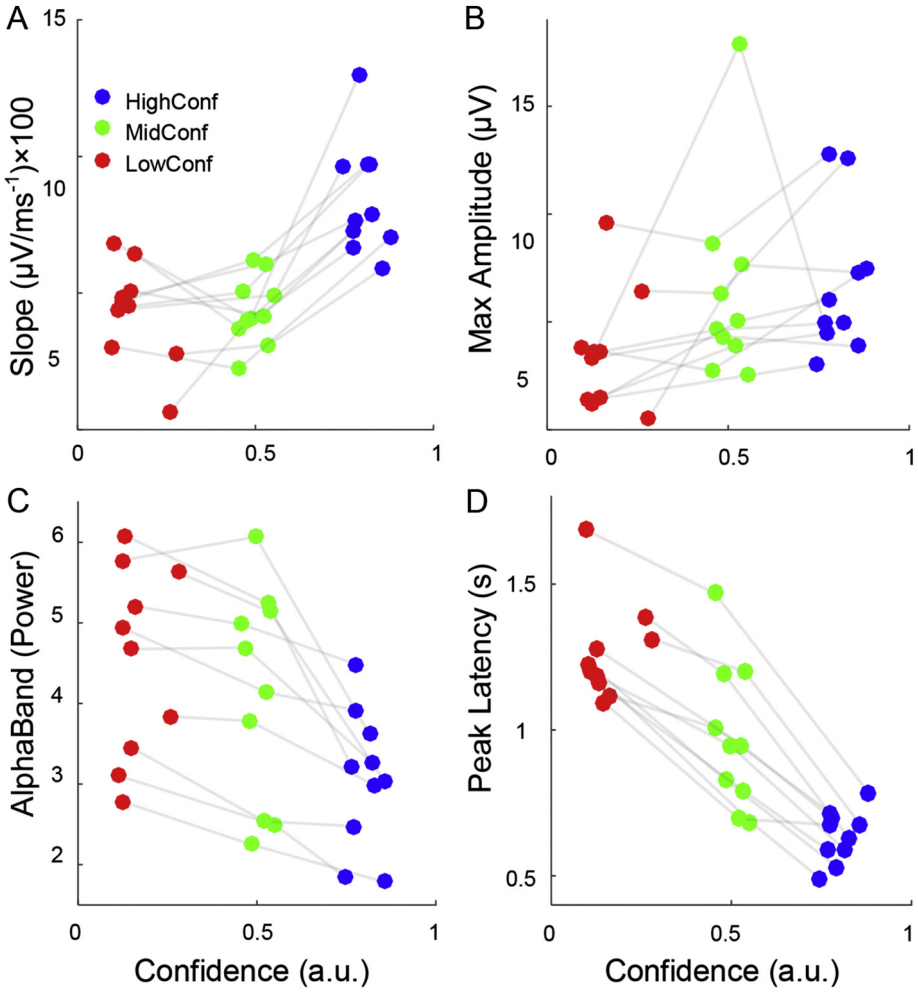

Fig. 4. EEG features. (A) The first feature was the slope of the signal from 300 ms after the onset of the stimulus until the time of the positive peak. The black line was the fitted line to data. Every colored dot represents a subject (n = 10). Black dots are related to the mean of feature values on every confidence level which also shows the relationship between the mean value of the features and the mean confidence levels. **(B)** The second feature was the maximum value on the signal 300 ms after the onset of the stimulus where the correlation is evident. **(C)** The third feature was the signal alpha band amplitude from 300 ms after the onset of the stimulus until the time of the maximum signal amplitude. There was a reverse correlation between this feature and the confidence value. **(D)** The fourth feature was the latency of the positive peak. This feature was the strongest EEG feature for confidence representation.

responses. Fig. 3D expresses that the ERPs of the three levels of confidence are independent of accuracy coding in the centro-parietal area and they are associated to a degree of certainty.

A more profound analysis in order to outcast any influence of other factors in discrimination of confidence level in the centro-parietal area, in addition to eliminating effects of coherence and accuracy, is the evaluation of the confidence signals with the same RT distribution of one level coherence. Here, we choose a Same RT subset of 12.8% and 6.4% coherencies (Zizlsperger et al., 2014) (see the method section). Since RT distribution can be varied in each level of confidence, we needed to decline the assumption that the distinction of the confidence levels was relative to the different RT distributions. Fig. 3E represents the ERP of the three levels of confidence in this condition. As is clear, the distinctions between confidence signals were rested in this analysis.

In the following, we evaluated different properties observed in the EEG signals as confidence features. We argue that these features are able to decode confidence levels properly. In addition to the mentioned factors, the recent studies revealed the relationship of the alpha band with the RT and motion strength (Kelly and O'Connell, 2013). We also assessed the alpha band as another possibility that may have a significant relation to confidence.

All the upcoming EEG analyses were accomplished on unfiltered data (Kelly and O'Connell, 2013) Fig. 4 shows the relation of the EEG features to confidence. The first feature (Fig. 4A) was the slope of the signal from 300 ms after the onset of the stimulus until the time of the signal positive peak. The extracted values corresponded to each confidence level is statistically different ($H(2) = 14.82$, $P < .001$). It is inevitable to consider the slope time latency for every trial dependently. The fitted line slope on a constant specific time (300–600 ms) for all the trials could not reveal a significant relationship with the confidence levels ($H(2) = 0.48$, $P = .79$).

Fig. 4B shows the second feature, the amplitude of the signals during the positive peak. The statistic test suggested that this feature was a slightly weaker representative of the confidence levels, as compared to the first one ($H(2) = 7.12$, $P = .02$). Note that the average value of the signal amplitude was independent of the confidence levels at 300 ms after the onset of the stimulus until the latency of the positive peak ($H(2) = 2.54$, $P = .28$).

The third feature was the alpha band of the signal from 300 ms after the onset of the stimulus until the time of the positive peak (Fig. 4C). Based on the statistics, this feature was stronger than the second feature but weaker than the first one ($H(2) = 8.51$, $P = .01$). Interestingly, the alpha band analysis on the onset of the stimulus to the time of the peak showed no significant relationship with confidence ($H(2) = 2.32$, $P = .31$).

As Fig. 4D represents, the strongest EEG feature was the latency of the signal positive peak ($H(2) = 23.1$, $P < .001$). This property was relatively a part of other features definition and affected their returned values. All the three other features were defined at the peak of the signal; the second feature extracted the value of the signal in this latency, while the first and third ones considered this time as their ultimate time point.

Despite considerable changes in early ERPs amplitudes, the first 200 ms of the signal conveyed insignificant information about the confidence levels. We analyzed the mean and max value of the signal amplitude across the levels of confidence in this period (150–250 ms) and observed no significant relationship ($H(2) = 1.23$, $P = .55$ and $H(2) = 1.98$, $P = .37$, respectively).

Furthermore, we analyzed data in the absence effect of coherence and RT. In the one level coherence analysis, we used 12.8%. First and fourth EEG feature is still able to represent different confidence levels ($H(2) = 6.29$, $P = .04$ and $H(2) = 10.01$, $P = .006$ respectively). For RT analysis, we selected a subset of data with the coherence of 12.8% and 6.4% (Zizlsperger et al., 2014) which have similar RTs. This analysis introduces the EEG latency as the confidence representative feature ($H(2) = 7.00$, $P = .03$).

Having analyzed subject based examination on the EEG features, here we evaluated confidence features by latency analysis. This analysis could introduce important time periods which could be considered crucial in the decision making and confidence formation process. Fig. 5A represents decoding analysis (Cichy et al., 2014; Karimi-Rouzbahani et al., 2017a, 2017b) of the all EEG data related to the three levels of confidence (see the method section). The highest accuracy belonged to 557 ms after the onset of the stimulus. In this time, the signals had the highest discrimination based on their confidence levels. In this way, it can be inferred that in this time, the signals contained the most pertinent information about the confidence levels. Obviously, the accuracy more than indicated chance level (based on three confidence level) could convey valuable information to confidence. Fig. 5B shows the same decoding analysis for EEG data of Same RT subset. In 583 ms after the onset of the stimulus, the decoding accuracy reaches to its maximum value which means in this time the signal conveys most related information to the confidence levels. Note results in Fig. 5 are the average of 200 runs in every step.

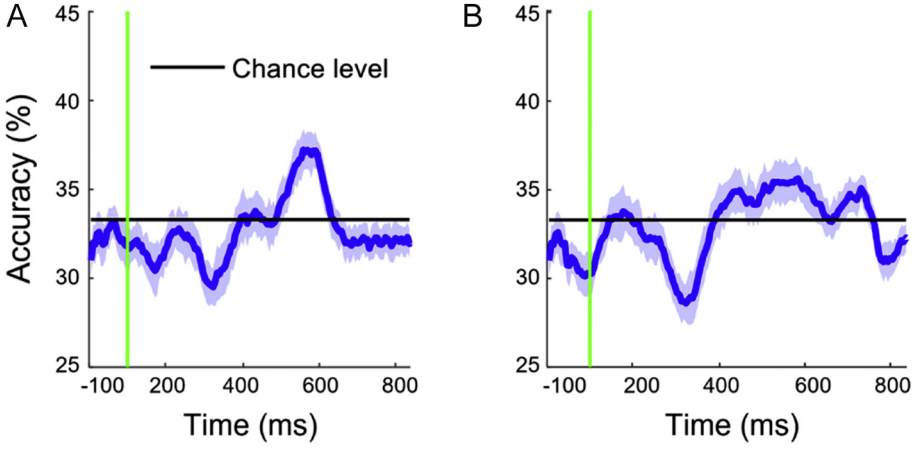

Fig. 5. Latency analysis of the extracted features. (A) Decoding analysis of the three confidence levels on EEG data. The signals in the 557 ms after the onset of the stimulus had the most discrimination. The black line indicated the chance level boundary (33.33%) while the green line specified the stimulus onset. The EEG signals conveyed information about the confidence levels when they showed a higher accuracy than the chance level. **(B)** Same analysis on the Same RT subset. Descriptions are the same as A. The signals reached their maximum separability in 583 ms after onset of the stimulus.

The observations in Fig. 5 suggested the importance of 500–600 ms period in the EEG signals which are in line with the P300 time interval.

Eye data features

Having discussed the EEG features, in this section, we also analyzed the eye data to evaluate whether there was any correlation between eye data parameters and confidence in order to extract possible features from these data as well. At first, we evaluated the pupil signals (pupil size over time) for the three levels of confidence. The Eyelink system, in addition to the pupil diameter, detects eye movement events such as fixation, saccade, blink and so on based on its embedded algorithm. These events could contain information about confidence.

Fig. 6A,B represents the pupil size behavior in the stimulus and response-locked trials for all trials. On the stimulus-locked plot, the confidence levels were not clearly distinct from each other. However, the response-locked analysis suggested that high confidence trials tended to have lower pupil size than the other two confidence levels. In this situation, the mean amplitude of the pupil signal seemed to have a reverse correlation with the level of confidence. However, this effect was not significant ($H(2) = 1.79$, $P = .41$). Yet, the pupil size at the time of response was able to differently represent the confidence levels ($H(2) = 18.50$, $P < .001$ see Fig. 7D). Moreover, the slope of the fitted line from the onset of the stimulus to response time could convey information about the confidence levels. This value was expected to be negative for high confidence trials and near zero for low confidence trials. The latency of the signal positive peak could express pertinent information to the confidence levels as well. In other words, high confidence pupil signals tended to reach their maximum value in an early representation of the stimulus while this time lasted until response time for low confidence ones.

Fig. 6C,D represent the same analysis as Fig. 6A,B for the Same RT subset. Statistical analysis on pupil size as the time of response showed no relationships to confidence levels ($H(2) = 2.28$, $P = .32$). However, the confidence information in this situation could be extracted by other features which we brought in follow.

The first eye data feature was quite similar to the first EEG feature (slope) except that the slope of the pupil size was calculated from the onset of the stimulus until response time (time of the saccade initiation headed to one of the target bars (Fig. 7A)). This feature's values are significantly different for confidence levels ($H(2) = 13.58$, $P = .001$).

The second feature for the eye data was the latency of the maximum

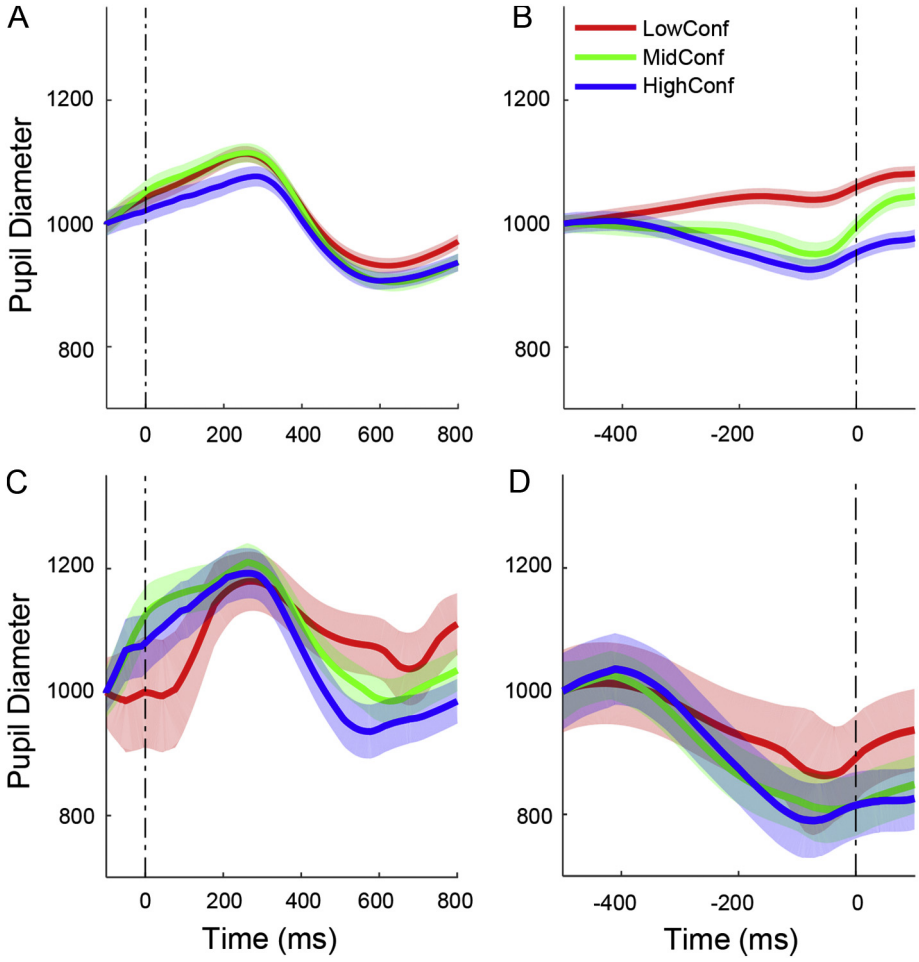

Fig. 6. Pupil signals for the three confidence levels. (A) The stimulus-locked signals which did not show specific discriminations based on the confidence levels. **(B)** The response-locked signals corresponding to the confidence levels were separated appropriately. In the both plots, the shaded error area corresponded to the SEM. blink events were removed; the signals were smoothed by 30 ms windows of the averaging filter. **(C)** Same analysis as A for Same RT subset. Descriptions are the same as A. pupil signals did not show pertinent information to the confidence levels. **(D)** Same analysis as B for one level coherence and Same RT subset. Descriptions are the same as B.

value for the pupil signal. This feature is the strongest feature among all eight proposed features ($H(2) = 28.09$, $P < .001$; Fig. 7B).

For the third eye data feature, the number of fixation events while the stimulus is represented has been considered (Navajas et al., 2014). It is important to note that the normalized number of fixations was measured as a mentioned feature. Without normalizations, low confidence trials tended to have more fixation number than high confidence ones due to slower response time. Summations of fixation events through stimulus representation were evaluated as well. This value had a significant correlation with the confidence level ($H(2) = 9.85$, $P = .007$). For comparison, it was necessary to compare this variable in the same amount of time. In this way, it could be inferred that high confidence level tends to fixate on more often rather than lower ones ($H(2) = 23.03$, $P < .001$; Fig. 7C). In other words, stimulus representation caused significantly a greater number of fixations in high confidence trials in comparison with lower confidence ones. Note that the *P*-value for the normalized fixation numbers was slightly smaller than that one for RT and confidence levels (for RT: $H(2) = 21.29$, $P < .001$). It means that our third eye data feature conveyed more related information than the RT itself. We further analyzed the mean values of pupil size and saccade speed of the three confidence levels and obtained no significant relationship between them ($H(2) = .98$, $P = .61$ and $H(2) = 1.97$, $P = .37$, respectively). The last feature is pupil size at the time of response (Fig. 7D) which we discussed earlier. Moreover, we analyzed the eye data features in one level coherence and Same RT subset. In the one level coherence analysis, while second and third features are able to significantly represent confidence levels ($H(2)=14.00$, $P < .001$ and $H(2) = 9.21$, $P = 0.01$ respectively), the remaining features – first and forth are able to weakly represent the confidence levels ($H(2) = 4.88$, $P = .09$ and $H(2) = 5.20$, $P = .07$). Same RT analysis shows the second eye data feature are still able to represent confidence levels ($H(2) = 8.11$, $P = .01$). (See Table C.1 in Appendix A section for post hoc tests).

Overall, based on the accomplished analysis in Figs. 4 and 7, the second feature for eye data (latency of the maximum value for the pupil signal) was the most demonstrative property among all the eight proposed features in the EEG and eye data. Table 1 shows the eight studied features with four being for the EEG and four being for the eye data. Employing the single trial analysis- as a more reliable analysis- we can investigate the feature representative capability even more precisely (Fig. 8A, Kruskal-Wallis test). Because we averaged on the subject data for every feature, we might lose valuable information in the averaging procedure; hence, evaluations Figs. 4 and 7 might not be completely reliable. Except for the MaxAMP, all other features are able to represent confidence levels significantly, in one level coherence analysis. In a stricter situation, the Same RT analysis shows the EEG latency is able to represent different confidence levels; all eye features except NumFix are also significantly confidence representative. Important to note, while the subjective analysis introduced only 2 out of our 8 features (EEG latency and Pupil Latency) as the confidence representative features, the single trial analysis revealed 4 out of 8 features are able to represent confidence in this intense situation (Same RT subset).

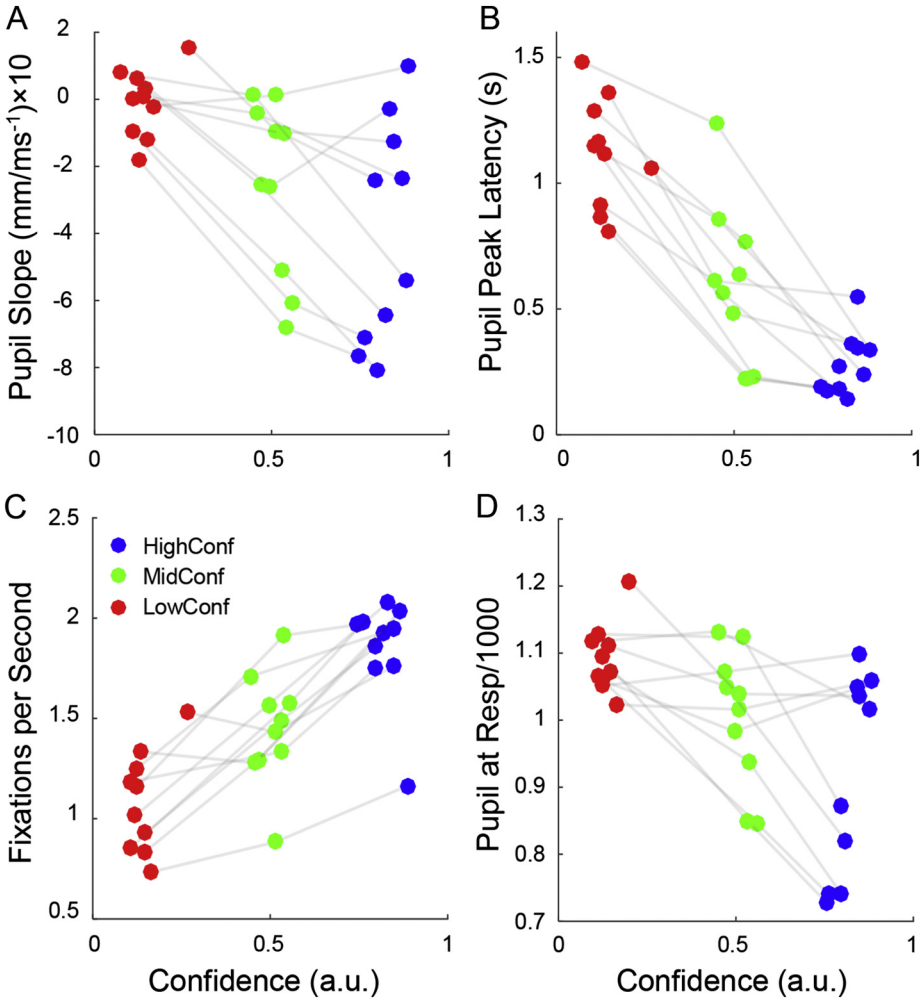

Fig. 7. Eye data features. (A) The first feature was the slope of the pupil signal from the onset of the stimulus until the time of saccade initiation. The black line was the fitted line to data. Every colored dot represents a subject (n = 10). Black dots are related to the mean of feature values on every mean confidence level. **(B)** The second feature was the latency of the positive peak in the pupil signal. This feature was the strongest feature for confidence representation. **(C)** The third feature was the normalized number of the fixation points through stimulus presentation; the number of fixations per second was extracted and analyzed as the eye data feature. **(D)** The forth feature was the pupil diameter at the time of response. Higher confidence was associated with lower pupil diameter at the time of response.

We also evaluated our features' potentials of confidence predictably in all trials. In this way, for every feature, we used an SVM classifier to detect 3 confidence levels (Fig. 8B). Features with more accurate results are more confidence representative. EEG latency is the best EEG feature and Pupil Latency is the best eye features while all the features is able to reach to better accuracy than the Decoding analysis (Fig. 5A). However, using all eye features (All Eye) and using all EEG and eye features (EEG&Eye) could lead to better representation of the confidence.

Moreover, our features were able to decently predict continuous values of confidence scaled from 0 to 1 (regression MSE with 10-fold cross validation: 0.108 ± 0.011 by the generalized regression neural network (GRNN)). This analysis indicates that the proposed features can recognize up to nine confidence levels properly.

POST-EXPERIMENT RESULTS

In this study, all the EEG analyses were achieved 300 ms after the onset of the stimulus due to the sensory-evoked potential at the early stimulus onset (200 ms). Similar studies (Kelly and O'Connell, 2013, 2015) have shown signal behavior in coherence levels which is slightly different from what we reported in Fig. 3B. The main difference is related to the positive peak around 200 ms after the onset of the stimulus. It is noteworthy that the mentioned studies used the continuous version of the RDM task where the subjects observed a zero-coherence motion before the coherent motion. The seamless transition prevents the sudden change in signals and thus this peak was not evident in this version. To establish the proof for our argumentation, we designed a continuous version of the RDM task. In this way, before observing any coherent motion, the subjects faced a 500 ms zero-coherent motion dot. With this variation, the reported effect was diminished and became comparable to the previous studies. The ERP signal related to high and low confidence levels in the continuous version of the RDM task is shown in Fig. 9A. Removing the sudden appearance stimulus could lead to the absence of 200 ms peak in the EEG signal. Yet we applied the classic version of our main paradigm because this version was previously exploited in EEG and eye tracking investigations and it was much more favored in perceptual decision making discussions than in the continuous ones.

All the EEG results were analyzed only in the stimulus-locked signals and we did not examine the response-locked signals due to the destructive effect of saccadic decision report on the amplitude of these signals (see discussion section). Previous studies have demonstrated that the decision signals reach a threshold at the moment of response in the centro-parietal area (O'Connell et al., 2012; Twomey et al., 2015). We reviewed this effect in our decision making signals and observed that the negative amplitude of the signal varied across coherence levels and the signals did not reach a constant level in response time (Fig. 9B). This issue has been stated to be affected by spatial overlapping with an area which is responsible for

Table 1. The extracted confidence representative features in the EEG and eye data.

	Feature number	Description	Feature code
EEG	1	Slope of the signal from 300 ms after onset of the stimulus until the latency of the signal's positive peak.	EEG Slope
	2	Maximum value of the signal at the time of positive peak 300 ms after onset of the stimulus.	EEG Max AMP
	3	Alpha band of signal from 300 ms after onset of the stimulus until the time of the positive peak of the signal.	Alpha Band
	4	Latency of the signal at the positive peak after 300 ms after onset of the stimulus.	EEG Latency
EYE	5	Slope of the pupil signal from onset of the stimulus until the main saccade initiation.	Pupil Slope
	6	Latency of the pupil signal at its positive peak.	Pupil Latency
	7	Normalized number of fixation events while showing the stimulus.	Num Fix
	8	Pupil diameter at the time of response.	Pupil at Resp

motoric actions (The frontal eye field (FEF) effect) (Baker et al., 2012). Thus, to resolve this observed phenomenon, the decision signals must be eradicated from this malicious effect.

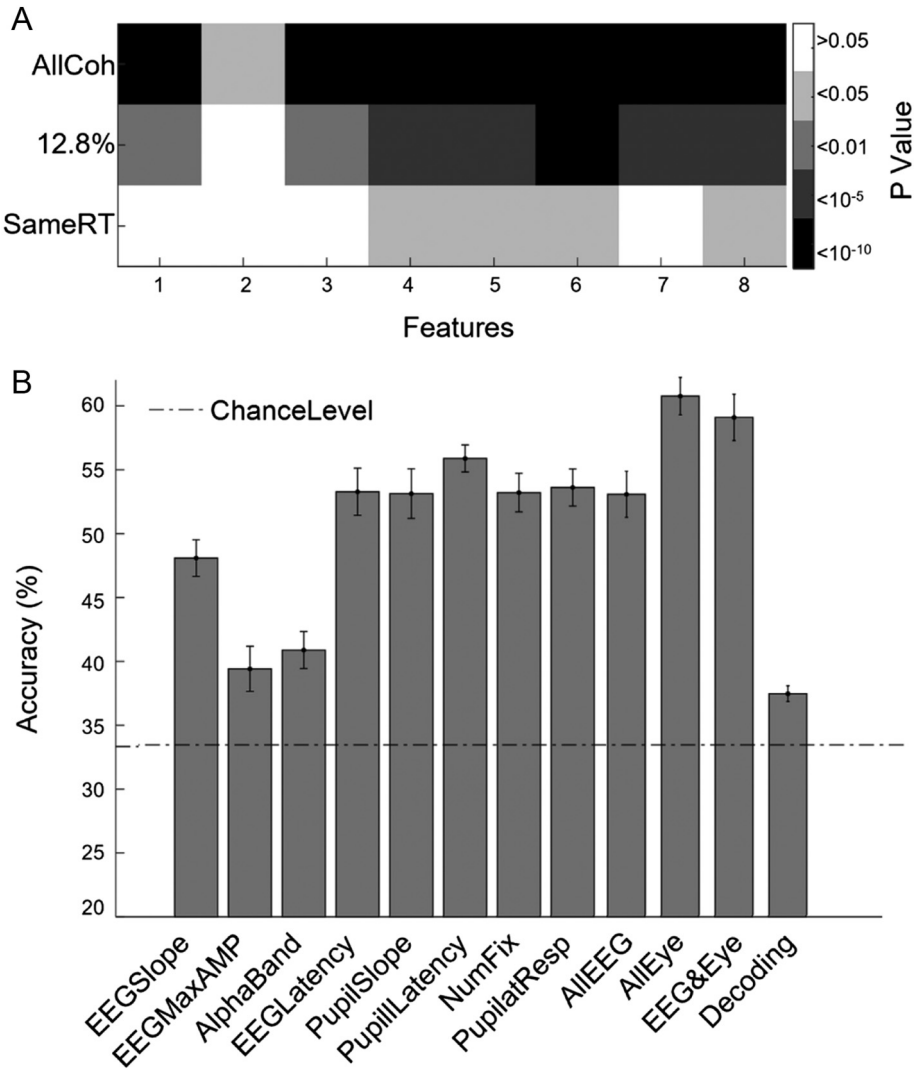

Fig. 8. Single trial analysis. (A) The statistical matrix of the extracted features based on different conditions by single trial analysis in different situations. The color bar represents different significant values (Kruskal Wallis test). **(B)** Features' classification analysis on all trials. The predictability of each feature alongside with combination of EEG and Eye feature have been shown. The Dashed line indicates the chance level performance. Error bars are the confidence interval of 95%. For A and B, Features have been specified by the corresponding number in Table 1.

The common method for removing the affection of one area on another area's signals (or overlap between areas of the brain) is the current source density (CSD) transformation (Kayser and Tenke, 2006; Kelly and O'Connell, 2013). To minimize the projection of motor preparation on the centro-parietal area, we employed the CSD transformation on the response aligned signals. After implementation of the CSD, the amplitude of the signals reached a negative certain value independent of coherence level (Fig. 9C). Note, we consider three coherence levels so that we averaged paired of the coherences respectively from high to low. However, the ERP amplitude continuously decreased until the decision report time and did not show ramping activity similar to previous studies (Kelly and O'Connell, 2013; Twomey et al., 2016) (Fig. 3B). In this way, we designed a new paradigm in which the subject needed to simultaneously report his or her decisions and confidence level by pressing a specific bottom out of four available keys (up or down and high confidence or low confidence). The intuition was to outcast the eye saccadic effect on decision signals in response time. In this version, the effect of the eye movement was eliminated properly. We considered only the highest and lowest coherence for a better representation. The signals showed ramping activity as a function of motion strength in the response-locked ERP (Fig. 9D). However, yet in response time, the signals did not reach a constant amplitude (decision criterion). This effect as described above was due to the influence of motor preparation on our signals (Frontocentral area). Our result in response aligned analysis was converted to CSD transformation which

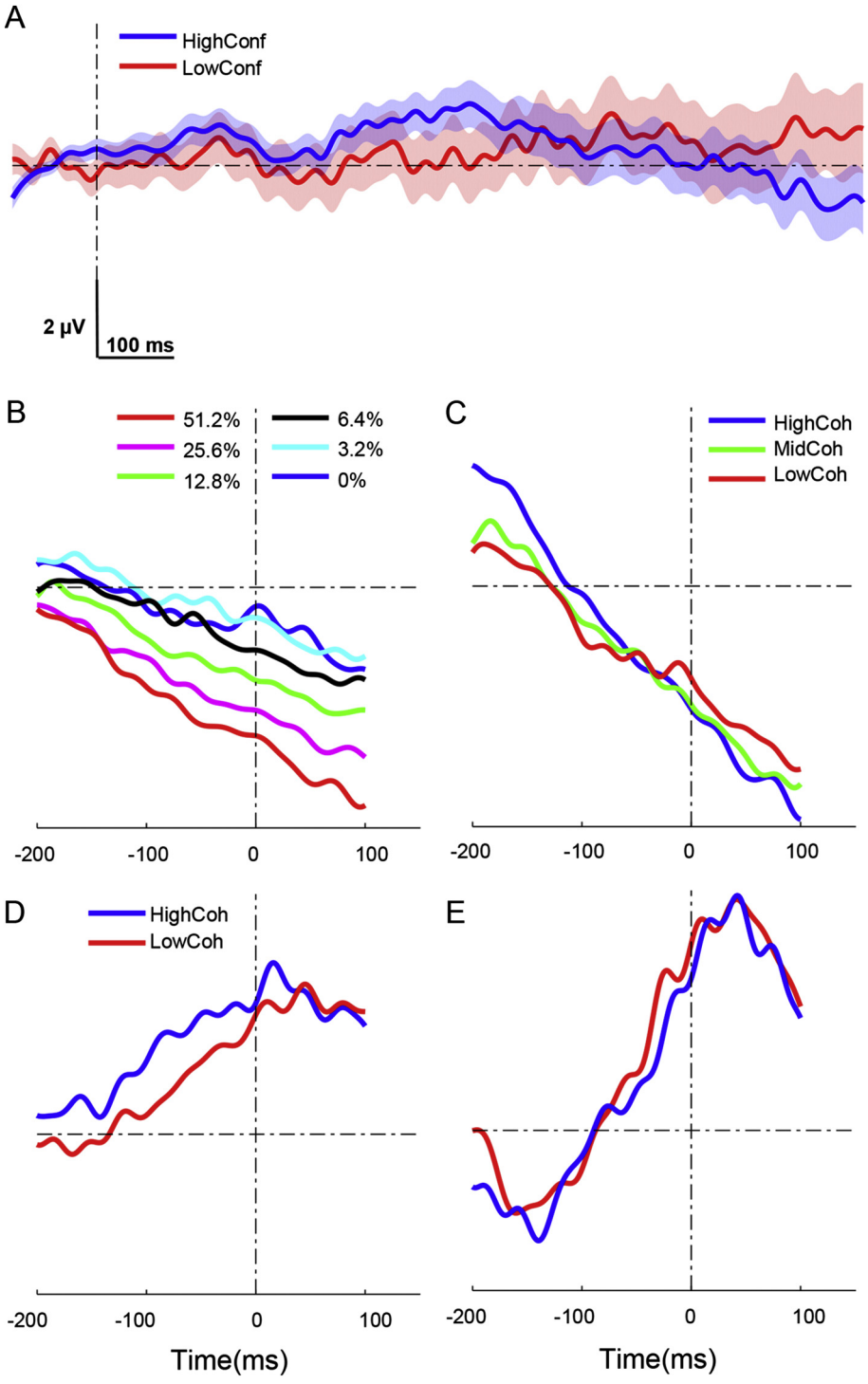

Fig. 9. Continuous version of RDM task and Signal behavior locked in response time. (A) The ERP of high and low confidence levels in the continuous version of RDM task without early peak around 200 ms after onset of the stimulus. Because of the continuous presentation of a stimulus, there was no sudden change in 200 ms in the ERP signal. (**B**) The ERP signal time locked to the response with no CSD transformation where the effect of saccadic eye movement was more intense in higher coherences. The reverse correlation between the amplitude of the signal and motion strength was obvious. **(C)** The ERP signals after applying the CSD where high coherence was the average of the two highest coherence levels of 51.2% and 25.6%, mid coherence was the average of 12.8% and 6.4% and low coherence was the average of the rest. These two waveforms reached the same amplitude in time of the report decision. **(D)** The signal behavior related to the second experiment in which the subjects reported their decision and confidence value by pressing a key (no eye movement). The negative amplitude was replaced with the ramping activities of the centro-parietal signals. Higher coherence (51.2%) had a higher amplitude than lower coherence (0%). **(E)** Applying a CSD transformation on the ERP of part C; the CSD transformation extracted the decision bound of the signals. Two signals reached a certation value.

can eliminate this effect sufficiently. The decisions criterion will be revealed after applying the CSD. Fig. 9E shows the footage.

DISCUSSION

The main novelty of this work was to propose eight confidence features in the EEG and eye data for a famous perceptual decision making task (RDM). We showed that the extracted features were significantly correlated to the confidence levels. This claim was confirmed on the subjective data (Figs. 4 and 7) and single trial analysis (Figs. 5 and 8).

Although, DDM fitted parameters have been utilized to interpret confidence in perceptual decision making in some studies (Ratcliff and Starns, 2009, 2013; Philiastides et al., 2014) however other works have emphasized that the classic DDM has some limitation in explaining the complexity of confidence (Moreno-Bote, 2010; Drugowitsch and Pouget, 2012; Yeung and Summerfield, 2012; Wei and Wang, 2015) and thus it might provide an estimation only under certain conditions. Yet, the DDM performs usually well in describing behavior in tasks when considering that confidence should reflect both the quality and quantity of evidence. Therefore, neither of the DDM parameters alone is adequate to define certainty of a subject. Consequently, here, we focused on all the DDM parameters and discussed their difference for the levels of confidence and not only with one of the parameters. In fact, low confidence was associated with low coherence (Palmer et al., 2005; Sadja et al., 2011; Philiastides et al., 2014; Van den Berg et al., 2016a, b). Moreover, as non-decision time relies heavily on data from high coherence, non-decision time may be unreliable for low confidence data. Alternatively, high confidence is associated with high coherence (Ratcliff and Starns, 2009, 2013). The decision bound relies heavily on data from low coherence, and thus decision bound may be unreliable for high confidence data.

In many experiments, confidence is commonly reported in discrete values via pressing multiple keys (Zizlsperger et al., 2014). What occurs between discrete values of confidence is not straightforwardly obtainable. By obtaining the continuous values, the confidence analysis could be made at any desired quintile. This capability was beneficial to our study. In addition, we wanted to analyze confidence features in eye data variables such as pupil size and saccadic parameters. Therefore, by the employment of the eye tracking system for reporting the decision and confidence level, we were able not only to record eye data through the task, but also to obtain the continuous values for confidence. Since we needed to use the eye tracker, all the EEG results were analyzed only in terms of the stimulus-locked signals and we did not discuss about the response-locked signals. The saccadic report might be detrimental for response-locked signal behavior in the centro-parietal area of the brain, especially in response time. Involving the eye controlling area of the brain in the decision making process (Gold and Shadlen, 2000) leads to the negative amplitude and slope in response aligned ERPs. This effect has an observable correlation with strengths of the motion in 300 ms before response execution (Fig. 9B). Hence, although the response-locked signals might convey information about confidence as some studies focused on these signals to investigate confidence (Boldt and Yeung, 2015; Tan et al., 2016), the destructive influence of the eye related motor response on our EEG signals locked to response time persuaded us not to consider any EEG analysis in this period.

EEG researches have shown that the amplitude of error trials is lower than that of correct ones; in this way, it is reasonable for the EPR amplitude related to the correct responses to be higher than all the trials (which containing error trials as well, Fig. 3A,D). In addition, high confidence ERP signal in correct trials decayed after its peak with a slower slope compared to the same ERP in Fig. 3A. Studies have revealed that high coherence error trials are followed by less RT compared to high coherence correct trials (Ratcliff and Rouder, 1998).; while mid and low coherence error trials follow longer RT. Since confidence has a strong correlation with motion coherence, this effect can be observed in decision confidence in which high confidence error trials have less RT than correct ones. Considering the fact that motor preparation in our task caused negative activity in the signals (Fig. 9A), the mentioned negative activity must be initiated sooner in error trials with high confidence than in correct trials. For this reason, it is expected to have a steeper slope after reaching the maximum amplitude in ERP for high confidence which contains error trials as well (Fig. 3A).

In overall, in this study, we evaluated the confidence correlation with the EEG and eye data and obtained eight features from these methods relative to the confidence. These features could estimate confidence values with approximately 10% error rate, meaning that we were able to recognize more than nine levels of confidence. The latency analysis revealed that the 500–600 ms interval after the onset stimulus could be an important time for the confidence process (Fig. 5). This time interval showed a significant relation to the extracted features and had maximum accuracy in decoding analysis. The famous P300 effect time interval properly included our extracted time period. Our features, once again, emphasized the important relation of this time to the confidence coding. We confirmed that there was the confidence pertinent information in this time which lied on different properties of the signal. Previous studies dealt with the only signal amplitude of this time period which was confirmed in our work as well (Fig. 5). We succeeded to recognize and introduce much more pertinent information to confidence rather than merely employing the signal amplitude. We additionally showed that this time interval was dependent on every single trial. In other words, the effect of P300 and formation of related information to confidence was not constant for every signal and trial. This time period might be employed for investigation in neurophysiology studies in decision or confidence formation and more precisely in molding studies. Since the EEG signal behavior is believed to mimic the same treatment as neural data (O'Connell et al., 2012), we assume that our extracted features might be evident in cell recording data as well.

ACKNOWLEDGMENTS

This work was partially supported by the Cognitive Sciences and Technologies Council under contract number 4608, and Institute for Research in Fundamental Sciences (IPM)-School of Cognitive Sciences (SCS). We are thankful to Sajjad Zabbah for his helpful discussions.

APPENDIX A

Table A.1. The pairwise multiple comparisons procedure (post hoc) for Kruskal–Wallis test relevant to the behavioral results.

Behavioral Parameters	Conditions	*P*-value
Discrimination threshold (α)	HL	.02
	HM	.82
	ML	.04
RT	HL	< .001
	HM	.01
	ML	.11

Table B.1. The pairwise multiple comparisons procedure (post hoc) for Kruskal–Wallis test relevant to the Model parameters.

DDM parameters	Conditions	AllCoh	12.8%
Drift rate	HL	< .001	.73
	HM	.04	.16
	ML	.23	.01
Threshold separation	HL	< .001	.40
	HM	.04	.32
	ML	.61	.01
Non-decisional constant	HL	< .001	.65
Time	HM	.04	.20
	ML	.67	.02
Starting point	HL	.01	.81
	HM	.04	.15
	ML	.81	.03

Table C.1. The pairwise multiple comparisons procedure (post hoc) for Kruskal–Wallis test relevant to the extracted features.

Features name	Conditions	AllCoh	12.8%	SameRT
EEG Slope	HL	<.001	.03	.23
	HM	<.001	.08	.51
	ML	.80	.83	.92
EEG Max AMP	HL	.02	.63	.88
	HM	.74	.92	.92
	ML	.07	.71	.90
Alpha Band	HL	.01	.11	.39
	HM	.09	.33	.75
	ML	.69	.86	.93
EEGLatency	HL	.00	.002	.02
	HM	.01	.08	.18
	ML	.05	.10	.30
PupilSlope	HL	<.001	.05	.20
	HM	.25	.69	.87
	ML	.05	.14	.35
PupilLatency	HL	.00	<.001	.01
	HM	.04	.07	.17
	ML	.02	.04	.11
NumFix	HL	<.001	.002	.30
	HM	.04	.06	.61
	ML	.05	.15	.88
Pupil at Resp	HL	<.001	.06	.27
	HM	.14	.58	.74
	ML	.07	.17	.29

REFERENCES

Bahrami B, Olsen K, Bang D, Roepstorff A, Rees G, Frith C, PTRS B. (2012) What failure in collective decision-making tells us about metacognition What failure in collective decision-making tells us about metacognition. Control :1350-1365.

Baker KS, Piriyapunyaporn T, Cunnington R. (2012) Neural activity in readiness for incidental and explicitly timed actions. Neuropsychologia 50:715-722 Available at https://doi.org/10.1016/j.neuropsychologia.2011.12.026.

Balakrishnan JD, Ratcliff R. (1996) Testing models of decision making using confidence ratings in classification. J Exp Psychol Hum Percept Perform 22:615-633 Available athttp://www.ncbi.nlm.nih.gov/pubmed/8666956.

Baranski JV, Petrusic WM. (1998) Probing the locus of confidence judgments: Experiments on the time to determine confidence. J Exp Psychol Hum Percept Perform 24:929-945 Available at http://doi.apa.org/getdoi.cfm?doi=10.1037/0096-1523.24.3.929.

Bogacz R, Brown E, Moehlis J, Holmes P, Cohen JD. (2006) The physics of optimal decision making: a formal analysis of models of performance in two-alternative forced-choice tasks. Psychol Rev 113:700.

Boldt A, Yeung N. (2015) Shared Neural Markers of Decision Confidence and Error Detection. J Neurosci 35:3478-3484 Available at http://www.jneurosci.org/cgi/doi/10.1523/JNEUROSCI.0797-14.2015.

Brainard DH, Vision S. (1997) The psychophysics toolbox. Spat Vis 10:433-436.

Churchland AK, Kiani R, Shadlen MN. (2008) Decision-making with multiple alternatives. Nat Neurosci 11:693-702.

Cichy RM, Pantazis D, Oliva A. (2014) Resolving human object recognition in space and time. Nat Neurosci 17:455-462 Available at: http://www.nature.com/articles/nn.3635.

Clauset A, Shalizi CR, Newman MEJ. (2009) Power-law distributions in empirical data. SIAM Rev 51:661-703.

de Gardelle V, Mamassian P. (2014) Does confidence use a common currency across two visual tasks? Psychol Sci 25:1286-1288.

de Lafuente V, Jazayeri M, Shadlen MN. (2015) Representation of Accumulating Evidence for a Decision in Two Parietal Areas. J Neurosci 35:4306-4318 Available at http://www.jneurosci.org/cgi/doi/10.1523/JNEUROSCI.2451-14.2015.

Delorme A, Makeig S. (2004) EEGLAB: an open source toolbox for analysis of single-trial EEG dynamics including independent component analysis. J Neurosci Methods 134:9-21.

Drugowitsch J, Pouget A. (2012) Probabilistic vs. non-probabilistic approaches to the neurobiology of perceptual decision-making. Curr Opin Neurobiol 22:963-969.

Drugowitsch J, Moreno-Bote R, Pouget A. (2014) Relation between belief and performance in perceptual decision making. PLoS One 9.

Fetsch CR, Kiani R, Newsome WT, Shadlen MN. (2014) Effects of Cortical Microstimulation on Confidence in a Perceptual Decision. Neuron 83:797-804 Available at https://doi.org/10.1016/j.neuron.2014.07.011.

Folke T, Jacobsen C, Fleming SM, De Martino B. (2016) Explicit representation of confidence informs future value-based decisions. Nat Hum Behav 1(2) Available at http://www.nature.com/articles/s41562-016-0002.

Gherman S, Philiastides MG. (2015) Neural representations of confidence emerge from the process of decision formation during perceptual choices. Neuroimage 106:134-143 Available at https://doi.org/10.1016/j.neuroimage.2014.11.036.

Gold JI, Shadlen MN. (2000) Representation of a perceptual decision in developing oculomotor commands. Nature 404:390.

Gold JI, Shadlen MN. (2002) Banburismus and the brain: Decoding the relationship between sensory stimuli, decisions, and reward. Neuron 36:299-308.

Gold JI, Shadlen MN. (2007) The neural basis of decision making. Annu Rev Neurosci 30:535-574 Available at http://www.annualreviews.org/doi/10.1146/annurev.neuro.29.051605.113038.

Hanks TD, Ditterich J, Shadlen MN. (2006) Microstimulation of macaque area LIP affects decision-making in a motion discrimination task. Nat Neurosci 9:682-689.

Hebart MN, Schriever Y, Donner TH, Haynes JD. (2016) The relationship between perceptual decision variables and confidence in the human brain. Cereb Cortex 26:118-130.

Heereman J, Walter H, Heekeren HR. (2015) A task-independent neural representation of subjective certainty in visual perception. Front Hum Neurosci 9:1-12 Available at http://journal.frontiersin.org/Article/10.3389/fnhum.2015.00551/abstract.

Huk AC, Shadlen MN. (2005) Neural activity in macaque parietal cortex reflects temporal integration of visual motion signals during perceptual decision making. J Neurosci 25:10420-10436 Available at http://www.jneurosci.org/cgi/doi/10.1523/JNEUROSCI.4684-04.2005.

Karimi-Rouzbahani H, Bagheri N, Ebrahimpour R. (2017) Average activity, but not variability, is the dominant factor in the representation of object categories in the brain. Neuroscience 346:14-28 Available at https://doi.org/10.1016/j.neuroscience.2017.01.002.

Karimi-Rouzbahani H, Bagheri N, Ebrahimpour R. (2017) Hard-wired feed-forward visual mechanisms of the brain compensate for affine variations in object recognition. Neuroscience 349:48-63 Available at https://doi.org/10.1016/j.neuroscience.2017.02.050.

Kayser J, Tenke CE. (2006) Principal components analysis of Laplacian waveforms as a generic method for identifying ERP generator patterns: I. Evaluation with auditory oddball tasks. Clin Neurophysiol 117:348-368.

Kelly SP, O'Connell RG. (2013) Internal and external influences on the rate of sensory evidence accumulation in the human brain. J Neurosci 33:19434-19441 Available at http://www.ncbi.nlm.nih.gov/pubmed/24336710.

Kelly SP, O'Connell RG. (2015) The neural processes underlying perceptual decision making in humans: Recent progress and future directions. J Physiol 109:27-37 Available at https://doi.org/10.1016/j.jphysparis.2014.08.003.

Kepecs A, Uchida N, Zariwala HA, Mainen ZF. (2008) Neural correlates, computation and behavioural impact of decision confidence. Nature 455:227-231.

Kiani R, Shadlen MN. (2009) Representation of confidence associated with a decision by neurons in the parietal cortex. Science 324:759-764 Available at: http://www.sciencemag.org/cgi/doi/10.1126/science.1169405.

Kiani R, Hanks TD, Shadlen MN. (2008) Bounded integration in parietal cortex underlies decisions even when viewing duration is dictated by the environment. J Neurosci 28:3017-3029 Available at http://www.jneurosci.org/cgi/doi/10.1523/JNEUROSCI.4761-07.2008.

Kiani R, Corthell L, Shadlen MN. (2014) Choice certainty is informed by both evidence and decision time. Neuron 84:1329-1342.

Kim JN, Shadlen MN. (1999) Neural correlates of a decision in the dorsolateral prefrontal cortex of the macaque. Nat Neurosci 2:176-185.

Kubanek J, Hill NJ, Snyder LH, Schalk G. (2015) Cortical alpha activity predicts the confidence in an impending action. Front Neurosci 9:1-15.

Lempert KM, Chen YL, Fleming SM. (2015) Relating pupil dilation and metacognitive confidence during auditory decision-making. In: & Pessiglione M, editor. PLoS One, 10. p. e0126588. Available at https://doi.org/10.1371/journal.pone.0126588.

Loughnane GM, Newman DP, Tamang S, Kelly SP, O'Connell RG. (2018) Antagonistic interactions between microsaccades and evidence accumulation processes during decision formation. J Neurosci 38:2163-2176 Available at http://www.jneurosci.org/lookup/doi/10.1523/JNEUROSCI.2340-17.2018.

Mazurek ME, Roitman JD, Ditterich J, Shadlen MN. (2003) A role for neural integrators in perceptual decision making. Cereb Cortex 13:1257-1269.

McSorley E, Lyne C, McCloy R. (2014) Dissociation between the impact of evidence on eye movement target choice and confidence judgements. Exp Brain Res 232:1927-1940 Available at http://link.springer.com/10.1007/s00221-014-3884-2.

Mognon A, Jovicich J, Bruzzone L, Buiatti M. (2011) ADJUST: An automatic EEG artifact detector based on the joint use of spatial and temporal features. Psychophysiology 48:229-240.

Moreno-Bote R. (2010) Decision confidence and uncertainty in diffusion models with partially correlated neuronal integrators. Neural Comput 22:1786-1811.

Navajas J, Sigman M, Kamienkowski JE. (2014) Dynamics of visibility, confidence, and choice during eye movements. J Exp Psychol Hum Percept Perform 40:1213-1227.

O'Connell RG, Dockree PM, Kelly SP. (2012) A supramodal accumulation-to-bound signal that determines perceptual decisions in humans. Nat Neurosci 15:1729-1735 Available at http://www.nature.com/articles/nn.3248.

Palmer J, Huk AC, Shadlen MN. (2005) The effect of stimulus strength on the speed and accuracy of a perceptual decision. J Vis 5:1.

Petrusic WM, Baranski JV. (2003) Judging confidence influences decision processing in comparative judgments. Psychon Bull Rev 10:177-183.

Philiastides MG, Heekeren HR, Sajda P. (2014) Human scalp potentials reflect a mixture of decision-related signals during perceptual choices. J Neurosci 34:16877-16889.

Purcell BA, Kiani R. (2016) Hierarchical decision processes that operate over distinct timescales underlie choice and changes in strategy. Proc Natl Acad Sci 113:E4531-E4540 Available at http://www.pnas.org/lookup/doi/10.1073/pnas.1524685113.

Quick RF. (1974) A vector-magnitude model of contrast detection. Kybernetik 16:65-67 Available at http://link.springer.com/10.1007/BF00271628.

Ratcliff R, McKoon G. (2008) The diffusion decision model: theory and data for two-choice decision tasks. Neural Comput 20:873-922.

Ratcliff R, Rouder JN. (1998) Modeling response times for decisions between two choices. Psychol Sci 9:347-356.

Ratcliff R, Rouder JN. (2000) A diffusion model account of masking in two-choice letter identification. J Exp Psychol Hum Percept Perform 26:127.

Ratcliff R, Smith PL. (2004) A comparison of sequential sampling models for two-choice reaction time. Psychol Rev 111:333.

Ratcliff R, Starns JJ. (2009) Modeling confidence and response time in recognition memory. Psychol Rev 116:59.

Ratcliff R, Starns JJ. (2013) Modeling confidence judgments, response times, and multiple choices in decision making: Recognition memory and motion discrimination. Psychol Rev 120:697.

Ratcliff R, Perea M, Colangelo A, Buchanan L. (2004) A diffusion model account of normal and impaired readers. Brain Cogn 55:374-382.

Reinagel P. (2013) Speed and accuracy of visual motion discrimination by rats. PLoS One 8.

Rohrbaugh JW, Donchin E, Eriksen CW. (1974) Decision making and the P300 component of the cortical evoked response. Percept Psychophys 15:368-374.

Roitman JD, Shadlen MN. (2002) Response of neurons in the lateral intraparietal area during a combined visual discrimination reaction time task. J Neurosci 22:9475-9489.

Sadja P, Philiastides MG, Heekeren H, Ratcliff R. (2011) Linking neuronal variability to perceptual decision making via neuroimaging. In: Ding M, & Glanzman DL, editors. Dyn brain an Explor neuronal Var its Funct significance. p. 214-232.

Samaha J, Iemi L, Postle BR. (2017) Prestimulus alpha-band power biases visual discrimination confidence, but not accuracy. Conscious Cogn 54:47-55 Available at https://doi.org/10.1016/j.concog.2017.02.005.

Shadlen MN, Kiani R. (2013) Decision making as a window on cognition. Neuron 80:791-806 Available at https://doi.org/10.1016/j.neuron.2013.10.047.

Shadlen NN, Newsome WT. (2001) Neural basis of a perceptual decision in the parietal cortex (area lip) of the rhesus monkey. J Neurophysiol 86:1916-1936.

Sutton S, Braren M, Zubin J, John ER. (1965) Evoked-potential correlates of stimulus uncertainty. Science 150:1187-1188.

Tan H, Wade C, Brown P. (2016) Post-movement beta activity in sensorimotor cortex indexes confidence in the estimations from internal models. J Neurosci 36:1516-1528 Available at http://www.jneurosci.org/cgi/doi/10.1523/JNEUROSCI.3204-15.2016.

Twomey DM, Murphy PR, Kelly SP, O'Connell RG. (2015) The classic P300 encodes a build-to-threshold decision variable. Eur J Neurosci 42:1636-1643.

Twomey DM, Kelly SP, O'Connell RG. (2016) Abstract and effector-selective decision signals exhibit qualitatively distinct dynamics before delayed perceptual Reports. J Neurosci 36:7346-7352 Available at http://www.jneurosci.org/cgi/doi/10.1523/JNEUROSCI.4162-15.2016.

Urai AE, Pfeffer T. (2014) An action-independent signature of perceptual choice in the human brain. J Neurosci 34:5081-5082.

Van den Berg R, Anandalingam K, Zylberberg A, Kiani R, Shadlen MN, Wolpert DM. (2016) A common mechanism underlies changes of mind about decisions and confidence. Elife 5:1-21.

Van den Berg R, Zylberberg A, Kiani R, Shadlen MN, Wolpert DM. (2016) Confidence is the bridge between multi-stage decisions. Curr Biol 26:3157-3168 Available at http://linkinghub.elsevier.com/retrieve/pii/S0960982216312064.

Voss A, Voss J. (2007) Fast-dm: A free program for efficient diffusion model analysis. Behav Res Methods 39:767-775.

Voss A, Nagler M, Lerche V. (2013) Diffusion models in experimental psychology: A practical introduction. Exp Psychol 60:385.

Wei Z, Wang X-J. (2015) Confidence estimation as a stochastic process in a neurodynamical system of decision making. J Neurophysiol 114:99-113.

White C, Ratcliff R, Vasey M, McKoon G. (2009) Dysphoria and memory for emotional material: A diffusion-model analysis. Cogn Emot 23:181-205.

Yeung N, Summerfield C. (2012) Metacognition in human decision-making: confidence and error monitoring. Philos Trans R Soc B Biol Sci 367:1310-1321 Available at http://rstb.royalsocietypublishing.org/cgi/doi/10.1098/rstb.2011.0416.

Zizlsperger L, Sauvigny T, Händel B, Haarmeier T. (2014) Cortical representations of confidence in a visual perceptual decision. Nat Commun 5 Available at http://www.nature.com/doifinder/10.1038/ncomms4940.

Zylberberg A, Fetsch CR, Shadlen MN. (2016) The influence of evidence volatility on choice, reaction time and confidence in a perceptual decision. Elife 5:1-31.

(Received 5 September 2018, Accepted 13 March 2019)
(Available online 21 March 2019)